

Supporting Information

Slow Magnetic Relaxation in structurally similar mononuclear 8-coordinate Fe(II) and Fe(III) compounds

Qian-Qian Su,^{a,†} Qiong Yuan,^{b,†} Xiao-Fan Wu,^{b,†} Si-Huai Chen,^c Jing Xiang,^{a,*} Xin-Xin Jin,^b Li-Xin Wang,^a Bing-Wu Wang,^{b,*} Song Gao,^{b,d,*} and Tai-Chu Lau^{e,*}

^a College of Chemistry and Environmental Engineering, Yangtze University, Jingzhou 434020, Hubei, P. R. China. E-mail: xiangjing@yangtzeu.edu.cn.

^b State Key Laboratory of Rare Earth Materials Chemistry and Applications and PKU-HKU Joint Laboratory on Rare Earth Materials and Bioinorganic Chemistry, Peking University, Beijing 100871, China. E-mail: gaosong@pku.edu.cn; Fax: (+86) 10-62751708.

^c School of Chemistry and Environmental Engineering, Wuhan Institute of Technology, Wuhan 430073, P. R. China

^d South China University of Technology, P. R. China

^e Department of Biology and Chemistry, Institute of Molecular Functional Materials, City University of Hong Kong, Tat Chee Avenue, Kowloon Tong, Hong Kong, China. E-mail: bhtclau@cityu.edu.hk

† These authors contribute equally.

Experimental

Materials and physical measurements

IR spectra were obtained as KBr discs using a Nicolet 360 FT-IR spectrophotometer. UV/vis spectra were recorded on a Perkin Elmer Lambda 19 spectrophotometer in 1 cm quartz cuvettes. Elemental analysis was performed using an Elementar Vario EL Analyzer. Cyclic voltammetry (CV) was performed with a CH Instruments Electrochemical Workstation CHI660C. A glassy carbon working electrode, a Pt wire counter electrode, and a saturated calomel electrode (SCE) as reference electrode were used. Variable-temperature magnetic susceptibility, *ac* magnetic susceptibility, and field dependence of magnetization were measured on a Quantum Design MPMS XL-5 SQUID system using powder samples made by the crystal samples. Background corrections were done by experimental measurement on the sample holder. The experimental susceptibilities were corrected for the diamagnetism of the constituent atoms (Pascal's tables).

X-ray crystallography

Crystals suitable for X-ray diffraction analysis were obtained for **1** and **2**. X-ray diffraction data were collected at 100 K on an Oxford CCD or a NONIUS Kappa CCD diffractometer using graphite-monochromated Mo K_{α} radiation ($\lambda = 0.71073 \text{ \AA}$) for **1** and **2** in the ω -scan mode. Absorption corrections were done by the multiscan method. The structures were resolved by the heavy-atom Patterson method or direct methods and refined by full-matrix least-squares using SHELX-97 and expanded using Fourier techniques. All non-hydrogen atoms were refined anisotropically. H atoms were generated by the program SHELXL-97. The positions of H atoms were calculated on the basis of riding mode with thermal parameters equal to 1.2 times that of the associated C atoms and participated in the calculation of final R-indices. Crystallographic data (excluding structure factors) for the structures in this paper have been deposited with the Cambridge Crystallographic Data Centre, CCDC, 12 Union Road, Cambridge CB21EZ, UK. Copies of the data can be obtained free of charge on quoting the depository numbers and CCDC 2011202-2011203 for these compounds.

Synthesis of $(\text{PPh}_4)_2[\text{Fe}^{\text{II}}(\text{L}^1)_2]$ (1**).** 2.1 equivalent of NaOH (15 mg, 0.38 mmol) in H_2O (1 mL) was added into a suspension of ligand 6,6'-bis(1H-tetrazol-5-yl)-2,2'-bipyridine (H_2L^1 , 50 mg, 0.17 mmol) in MeOH (15 mL) and solution was cooled down to 0 °C. A solution of $\text{Fe}(\text{ClO}_4)_2 \cdot 6\text{H}_2\text{O}$ (39 mg, 0.11 mmol) in MeOH (10 mL) was also cooled down to 0 °C and then slowly added into the solution of L^1 . Then mixed solution was retained at 0 °C for 24 h. The solvent was removed under reduced pressure and the solid obtained was dissolved in H_2O (15 mL). PPh_4Cl (200 mg, 0.53 mmol) was added into the red aqueous solution and red precipitates were formed immediately, which were collected by filtration and the solid was air-dried. Red needle crystals suitable for X-ray crystallography were obtained by slow diffusion of diethyl ether into a MeOH solution of **1**. Yield: 36 mg, 25%, on the basis of $\text{Fe}(\text{ClO}_4)_2 \cdot 6\text{H}_2\text{O}$. Elemental analysis of $\text{C}_{72}\text{H}_{52}\text{FeN}_{20}\text{P}_2$: *calcd*: C 65.76, H 3.99, N 21.30%; *found*: C 65.60, H 3.96, N 21.42; Selected IR spectra (KBr, cm^{-1}): 3392 (m), 3058 (w), 1602 (m), 1573 (m), 1438 (s, tz), 1380 (w), 1259 (w), 1168 (m), 1108 (s), 1051 (w), 997 (m), 813 (m), 757 (m), 725 (s), 688 (m), 632 (w), 528 (s), UV-vis (CH_3CN , 298 K), λ_{max} , nm (ϵ , $M^{-1} \text{ cm}^{-1}$): 246sh (51160), 267sh (25050), 274sh (20740), 316 (21790), 324 (22310).

Synthesis of $(PPh_4)[Fe^{III}(L^1)_2]$ (2**).** A MeCN solution (2 mL) of $(NH_4)_2[Ce(NO_3)_6]$ (148 mg, 0.27 mmol) was slowly added into a MeCN solution (2 mL) of **1** (350 mg, 0.27 mmol). The solution immediately changed to orange with formation of the orange precipitate. The reaction mixture was further stirred at RT for 1 h. The solid was collected by removing the solvent under reduced pressure, washed with water (3×3 mL), and air-dried. Yield: (260 mg, 98%). Red needle crystals suitable for X-ray crystallography were obtained by slow diffusion of diethyl ether into a MeOH solution of **2**. Elemental analysis of $C_{48}H_{32}FeN_{20}P$: *calcd*: C 59.09, H 3.31, N 28.71%; *found*: C 59.12, H 3.35, N 28.85%; Selected IR spectra (KBr, cm^{-1}): 3434 (w), 3139 (w), 1612 (m), 1577 (m), 1540 (w), 1484 (w), 1454 (s, tz), 1386 (w), 1267 (w), 1178 (w), 1157 (w), 1108 (s), 1014(w), 814 (m), 755 (m), 723 (m), 692 (m), 632 (w), 528(s). UV-vis (CH_3CN , 298 K), λ_{max} , nm (ϵ , $M^{-1} cm^{-1}$): 267sh (38640), 274sh (36000), 320 (24820), 480 (450).

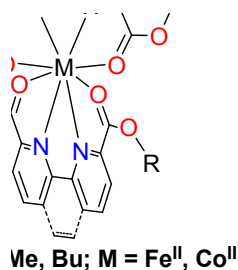


Fig. S1 The structures of 8-coordinate Fe(II) and Co(II) compounds with neutral ester ligands.

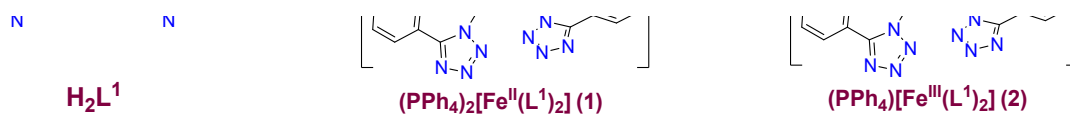


Fig. S2 Synthetic route for 8-coordinate Fe(II) (**1**) and Fe(III) (**2**) compounds.

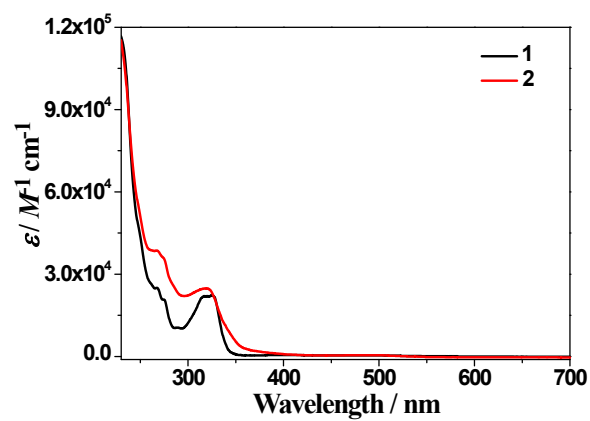


Fig. S3 The UV/vis spectra of **1** and **2** in CH₃CN.

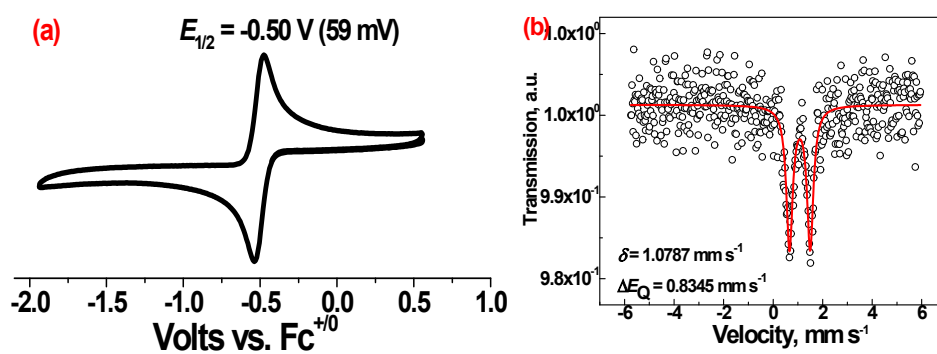


Fig. S4 (a) Cyclic voltammogram of **1** in 0.1 M [ⁿBu₄N]PF₆ MeCN solution with scan rate = 100 mV s⁻¹. (b) Mössbauer spectrum of **1** at 260 K.

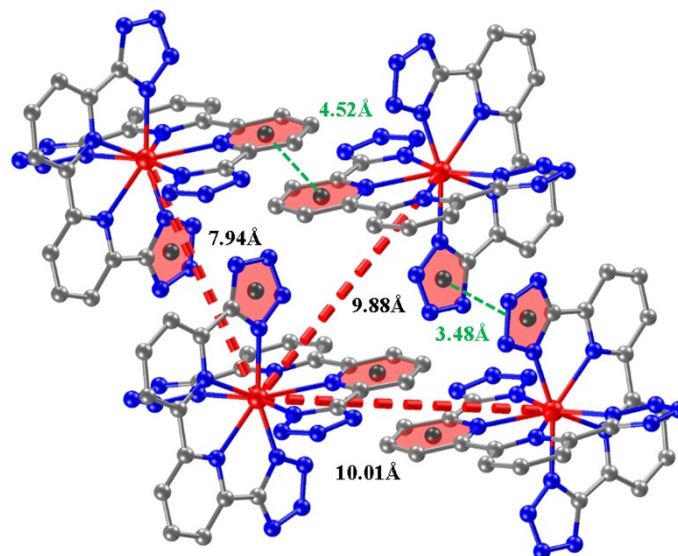


Fig. S5 The $\pi \cdots \pi$ stacking interactions in **2**.

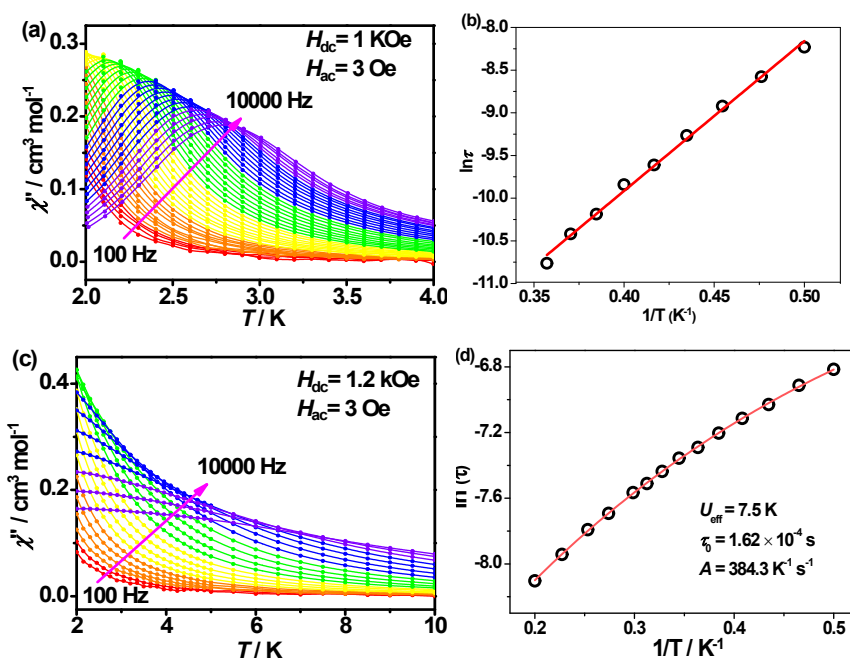


Fig. S6 (a) Temperature dependence of out-of-phase (χ'') signal of the ac magnetic susceptibility for **1** ($H_{dc} = 1.0$ kOe and $H_{ac} = 3$ Oe). (b) The $\ln(\tau)$ vs. $1/T$ plot for **1** and the red line is the best fitting Arrhenius plot. (c) Temperature dependence of out-of-phase (χ'') signal of the ac magnetic susceptibility for **2** ($H_{dc} = 1.2$ kOe and $H_{ac} = 3$ Oe). (d) The $\ln(\tau)$ vs. $1/T$ plot for **2** and the red line is fitted by Orbach and direct mechanisms.

Table S1. Crystal data and structure refinement details for compounds **1** and **2**.

	1	2
Formula	C ₇₂ H ₅₂ FeN ₂₀ P ₂ •4CH ₃ OH	C ₄₈ H ₃₂ FeN ₂₀ P•CH ₃ OH
<i>Mr</i>	1443.29	1007.80
<i>T</i> /K	173 (2)	100.0 (1)
Crystal syst	Triclinic	Monoclinic
Space group	P-1	P2 ₁ /n
<i>a</i> /Å	14.0404 (4)	19.6724 (7)
<i>b</i> /Å	14.6915 (4)	7.9390 (2)
<i>c</i> /Å	19.3746 (6)	30.9185 (10)
α , (°)	110.013 (2)	/
β , (°)	103.982 (2)	94.775 (3)
γ , (°)	95.7680 (10)	/
<i>V</i> / Å ³	3569.59 (19)	4812.1 (3)
<i>Z</i>	2	4
ρ_{calcd} , Mg m ⁻³	1.343	1.391
F(000)	1504	2076
Collected refl.	32276	21668
Unique refl.	14328	8490
<i>R</i> (int)	0.052	0.064
<i>R</i> ₁ , <i>I</i> > 2 σ (<i>I</i>)	0.113	0.055
w <i>R</i> (all)	0.343	0.197
GOF	1.20	0.67
No.of par.	937	651

Table S2. The selected bond lengths (Å) for **1** and **2**.

	1	2
Fe1-N1	2.386(4)	2.132(3)
Fe1-N5	2.483(4)	2.346(3)
Fe1-N6	2.474(5)	2.362(3)
Fe1-N10	2.407(5)	2.126(3)
Fe1-N11	2.369(5)	2.153(4)
Fe1-N15	2.489(5)	2.328(3)
Fe1-N16	2.492(5)	2.337(3)
Fe1-N20	2.381(5)	2.158(3)